applied sciences

MDPI

Article

An Optimal Resource Allocation Scheme with Carrier Aggregation in 5G Network under Unlicensed Band

Jin Li [1,2], Tong Zheng [1,2,*], Wenyang Guan [1,2] and Xiaoqin Lian [1,2]

[1] School of Artificial Intelligence, Beijing Technology and Business University, Beijing 100048, China; jinli@btbu.edu.cn (J.L.); 20151005@btbu.edu.cn (W.G.); lianxq@th.btbu.edu.cn (X.L.)
[2] Key Laboratory of Industrial Internet and Big Data, China National Light Industry, Beijing Technology and Business University, Beijing 100048, China
* Correspondence: 20211206@btbu.edu.cn

Abstract: Carrier aggregation (CA) technology in the Fifth-Generation (5G) network can be considered as a major feature for high-rate data services, which can be combined with the concept of 5G in unlicensed band (5G-U) for data offloading to further enhance the efficiency of the scarce licensed spectral resource. However, the introduction of cellular services in an unlicensed spectrum can force unlicensed band users to silent mode. Meanwhile, the coexistence among different radio access technologies operating on the same frequency band is a complex issue, especially considering the requirement diversity of quality of service (QoS) in networking. In this paper, we propose an optimal resource allocation mechanism to maximize system performance satisfaction for multiple types of services with different QoS requirements in the 5G-U network with a CA feature to address the challenge. Additionally, the performance of services in Wi-Fi system is protected by reserving the minimum spectrum resource when offloading for the 5G-U network. Analytical results on the mean ergodic achievable rate of Wi-Fi services and the mean packet delay of 5G services are provided to maximize the system performance satisfaction. Numerical results demonstrate the effectiveness of the proposed algorithm, wherein optimal spectrum and power allocation can contribute to the maximum system satisfaction in a 5G-U network with a CA feature.

Keywords: 5G-U; carrier aggregation; ergodic achievable rate; MAC mechanism; mean packet delay; optimal resources allocation; QoS; system satisfaction

check for updates

Citation: Li, J.; Zheng, T.; Guan, W.; Lian, X. An Optimal Resource Allocation Scheme with Carrier Aggregation in 5G Network under Unlicensed Band. *Appl. Sci.* **2023**, *13*, 10638. https://doi.org/10.3390/app131910638

Academic Editor: Amalia Miliou

Received: 3 August 2023
Revised: 19 September 2023
Accepted: 23 September 2023
Published: 24 September 2023

Copyright: © 2023 by the authors. Licensee MDPI, Basel, Switzerland. This article is an open access article distributed under the terms and conditions of the Creative Commons Attribution (CC BY) license (https://creativecommons.org/licenses/by/4.0/).

1. Introduction

To accommodate the quality-of-service (QoS) requirement diversity including high throughput, low latency of proliferation of data-hungry devices and applications in recent years, new advanced features have been added to the Fifth-Generation (5G) technology. Meanwhile, 5G has been proposed as the key technology to unlock the potential in realizing the Industry 4.0 communication goals [1]. In 5G network, one main challenge is to support 10 Gbps data rate of transmission for low-mobility users at the same time as 1 Gbps for high-mobility users, which requires a hundreds of MHz carrier bandwidth. Nevertheless, it is impossible to achieve a contiguous spectrum band with such a wide bandwidth on the licensed spectrum [2,3].

Then, the scarcity of licensed spectra for cellular network forces wireless industries to utilize the unlicensed bands, such as 5G in unlicensed band (5G-U) [4,5]. As the most important candidates of 5G-U, industrial, scientific and medical (ISM) radio bands such as 6GHz bands for wireless fidelity (Wi-Fi) 6 have been considered [6]. It is well known that the utilization of Wi-Fi systems for offloading data traffic from macrocell BSs has achieved a remarkable performance gain [7]. Furthermore, the main challenge to utilize 5G-U is that the cellular service users can be allocated to an unlicensed spectrum and force the unlicensed band users to silent mode due to the carrier sense multiple access with collision

avoidance (CSMA/CA) mechanism utilized by the traditional unlicensed system, while there is no carrier sensing before cellular services on unlicensed band transmission [8,9]. Meanwhile, Ref. [10] shows that the introduction of cellular services in unlicensed bands can significantly degrade the unlicensed band users due to the interference, while the cellular service performance is nearly unchanged, which makes the cooperative operation for 5G-U system a challenge but essential and necessary [5].

On the other hand, the 3rd Generation Partnership Project (3GPP) introduces carrier aggregation (CA) as one of the most important features in Rel-10, and subsequently enhances in Rel-11 and Rel-12. CA technology enables the aggregation of multiple resource blocks (RBs) from different component carriers (CCs) into a virtual carrier with larger bandwidth to achieve higher throughput and lower latency [11,12]. Without a doubt, as a remedy with the understanding that it cannot be used to achieve the needed bandwidth for the currently allocated licensed frequency spectrum, CA is introduced as one of the most momentous features in 5G networks [13,14].

However, it is advantageous while challenging to consider the 5G-U network with the CA feature, which requires elaborately designed system operation. In [15], the authors proposed optimum joint CC selection and RB allocation schemes to maximize the average throughput of users and satisfy the delay constraint of users. However, as one of the main characters of the 5G network, the diversity of QoS requirement is not considered in this paper. Then, in [16], the authors proposed the first joint CC selection and RB allocation scheme while optimizing user equipment (UE)'s power and rate and simultaneously taking delay constraint into consideration. However, multiple types of services in the 5G-U need to be analyzed based on their own characteristics and variable QoS requirements. As one of the most important performance metrics to evaluate the coexistence performance of multiple radio access technologies, outage probability in coexisting subnetworks is derived based on the primary and secondary cell association metric in this paper. Also, to meet the QoS requirements of various services for network performance at the system level, system satisfaction of QoS should be taken into account. In [17], the authors compared throughput fairness among UEs in the cell, although without considering the variable QoS requirements. Therefore, we formulate the system satisfaction maximization problem based on the user satisfaction ratio of each service type to the QoS requirement with outage probability as constraint. Moreover, to flexibly modify resource allocation to each service type based on the interest of the system operator, a system-level bias is given in the problem formulation part.

In the CA mode of operation, we utilize the Voronoi tessellation technique for CC allocation and primary CC (PCC) selection. Compared with the most popular two-dimensional hexagonal grid model, Voronoi tessellation is more suitable for practical cellular networks. Furthermore, aggregate characteristics of the Voronoi diagram in the Poisson–Voronoi (PV) system show superiority in analyzing networks [18]. Meanwhile, the efficient utilization of limited resources has been a major issue in wireless communication systems. In [19], a new dynamic CA scheduling scheme to improve the energy efficiency of uplink communications is proposed. In [20], carrier price per unit bandwidth is used to allocate multiple carrier resources optimally among users in their coverage area while giving the user the ability to select one of the carriers to be the primary carrier and the rest to be secondary carriers. Nevertheless, the integration of 5G-U and CA technology issues a challenge to existing networks, which cannot be addressed by the currently proposed schemes. In [12,21], Q-learning and double Q-learning methods are used for carrier selection and discontinuous transmission under efficient coexistence of 5G and Wi-Fi in unlicensed spectrum bands. However, existing studies represented by [12,21] did not consider multiple types of services in LTE-Advanced (LTE-A), which has already been one of the most fundamental and important network environments.

In this paper, we propose an optimal resource allocation mechanism to maximize system satisfaction under the constraints of variable QoS requirements for multiple types of services and outage probability thresholds in 5G-U networks with a CA feature. Firstly,

PCC and secondary CC (SCC) are selected optimally among all the aggregated CCs for different service types based on carrier quality and service type characteristics. Secondly, the outage probability for each service type is derived. Thirdly, the reserved unlicensed spectrum for rate-sensitive service is minimized to satisfy QoS requirement. Fourthly, mean packet transmission delay for delay-sensitive service is analyzed by the M/G/1 queue modeled in the corresponding user equipment (UE). Lastly, system satisfaction utility function is formulated and maximized with variable QoS requirements satisfied for different service types. Moreover, to flexibly modify resource allocation to each service type based on the interest of the system operator, a system-level bias is given in the problem formulation part. The numerical results reveal the superior effectiveness of the proposed scheme. The main contributions of this paper are listed as follows: 1: The RB resource allocation problem is turned into an UE aggregation problem for each CC and is then solved by utilizing the Voronoi tessellation properties. 2: The reserved unlicensed spectrum minimization problem is formulated and solved to protect the unlicensed band UE. 3: The mean packet transmission delay is derived for the delay-sensitive UE. 4: A system satisfaction maximization problem is formulated to take variable QoS requirements into one evaluation system and be maximized by optimally allocating spectrum and power resources. The notations in this paper are specified in Table 1.

Table 1. Notation definition.

Parameter	Definition
CA	Carrier aggregation
5G-U	5G in Unlicensed band
QoS	quality of service
CSMA/CA	carrier sense multiple access with collision avoidance
RBs	resource blocks
CCs	component carriers
UE	user equipment
PCC	primary CC
SCC	secondary CC
G	a graph represent the network
MBS	macrocell base station
M	set of M MBSs
AP	access point
S	set of S small cell APs
W	set of W Wi-Fi APs
U	set of U UE
δ_m	intensity of MBSs
δ_s	intensity of small cell APs
δ_w	intensity of Wi-Fi APs
δ_u	intensity of UE
D_t	delay threshold for delay-sensitive service
C_t	rate threshold for rate-sensitive service
ψ_d	association bias with small cell
ψ_r	association bias with Wi-Fi
ψ_u	association bias

Table 1. *Cont.*

Parameter	Definition
p_{iu}^{r}	received power at UE u from AP i
p_{iu}^{t}	transmit power from node i to node u
g_{iu}	channel gain
d_{iu}	distance between node i and node u
V_i	Voronoi cell i
$\mathbf{U}_i$	set of UEs associated with the AP i
N^I	the number of APs from set I
N^J	the number of APs from set J
d_{iu}	distance from u to i
d_{ju}	distance from u to j
λ_I	density of APs from I
λ_J	density of APs from J
CDF	cumulative distribution function
SINR	signal-to-interference-plus-noise
β	threshold for the received SINR
$\mathbf{Ic}_i$	co-channel interference power set
σ^2	white Gaussian noise
$\mathbf{\Phi}$	interference set
C_w	mean ergodic achievable rate
b_w	virtual carrier bandwidth for Wi-Fi AP to UE
p_w^t	transmit power for Wi-Fi AP to UE

The rest of this paper is organized as follows. In Section 2, we review the related literature. In Section 3, we describe the system model for the 5G-U network with a CA feature. In Section 4, we present the problem formulation to maximize system satisfaction with performance guarantee for a Wi-Fi system in 5G-U. In Section 5, we evaluate the effectiveness of the proposed algorithm by showing numerical results, followed by the discussion and presentation of future work in Section 6.

2. Related Literature

In [8], the total throughput of both downlink and uplink in 5G New Radio (5G NR) in an unlicensed channel spectrum is maximized by jointly optimizing the time and power allocation during the maximum channel occupation time duration while ensuring a fair coexistence with Wi-Fi. Meanwhile, previous research [22] derives explicit expressions of the maximum total network effective throughput and the corresponding optimal initial backoff window sizes of Wi-Fi and NR-unlicensed nodes. However, throughput is the only network performance metric considered in these papers and it leads to the preference for offloading the cellular traffic and best-effort transmissions by the Wi-Fi system. In [23], the authors investigate a 5G network with virtual network function-based reusable functional blocks and the total cost of the network is minimized by two algorithms derived by the authors. In [24], recent advances in technical standards and critical enabling techniques were reviewed. Moreover, the authors proposed and analyzed a novel hardware reuse and multiplexing solution to facilitate cost-effective and energy-efficient UE design. The authors in [13] provided an overview of CA, which is visualized as critical for 5G and upcoming networks. In [25], the transmission space was divided into two subspaces to allow for the coexistence of cellular users, Internet of Things devices, and Wi-Fi users. Meanwhile,

the cellular system throughput is maximized via the joint power and subchannel allocation under the interference constraint. Ref. [26] made a single-fed dual-band circular polarized dielectric resonator antenna for dual-function communication, which is a decent candidate for a global positioning system and wireless local area network. However, as the most distinguishing feature, variable QoS requirements for multiple types of services are not considered in these existing works, which requires a more efficient coexistence mechanism based on the network performance, and this need motivates this paper.

3. System Model

In this paper, we construct a heterogeneous 5G network under an unlicensed band with a CA feature, which can be represented by a graph $\mathbf{G}(\{\mathbf{M}, \mathbf{S}, \mathbf{W}\}, \mathbf{U})$. In G, $\mathbf{M} = \{m_1, \ldots, m_M\}$ is the set of M macrocell base stations (MBSs), $\mathbf{S} = \{s_1, \ldots, s_S\}$ is the set of S small cell access points (APs) and $\mathbf{W} = \{w_1, \ldots, w_W\}$ is the set of W Wi-Fi APs. $\mathbf{U} = \{u_1, \ldots, u_U\}$ is the set of U UE. The nodes from M, S, W and U are arranged according to Poisson Point Processes (PPPs) with intensities δ_m, δ_s, δ_w and δ_u in the Euclidean plane, respectively.

In a 5G network with a CA feature, RBs from different CCs are aggregated and utilized by access points (APs) based on carrier quality and QoS type. Moreover, data services are classified into delay-sensitive service and rate-sensitive service with corresponding QoS requirements, where D_t is the delay threshold for delay-sensitive service and C_t is the rate threshold for rate-sensitive service. The UE in delay-sensitive service is associated with small-cell APs in 5G and 5G-U with bias ψ_d, while the UE in rate-sensitive service is associated with Wi-Fi APs in unlicensed band with bias ψ_r, which means UE bias $\psi_u = \{\psi_d \cup \psi_r\}$. To protect the performance of Wi-Fi UE from the 5G-U UE, the minimum unlicensed spectrum resource is reserved based on the QoS requirement of rate-sensitive UE, as shown in Figure 1.

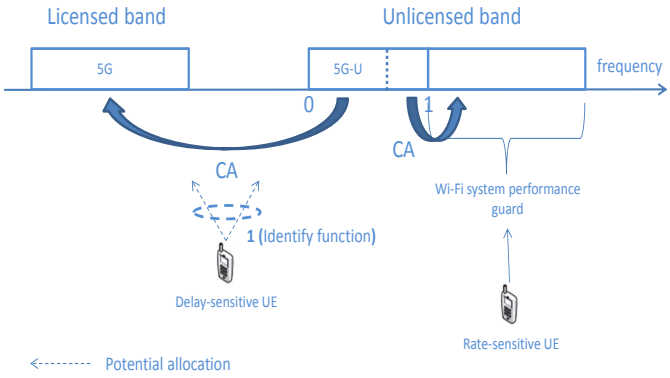


Figure 1. An illustration of 5G network under unlicensed band with CA feature.

In this paper, we adopt the Rayleigh fading channel model, which results in a random channel power gain in exponential distribution with unit mean [27]. Thus, the received power p_{iu}^r at UE u from AP i is shown as

$$p_{iu}^r = p_{iu}^t g_{iu} d_{iu}^{-\alpha}, \qquad \forall i \in \mathbf{S} \cup \mathbf{W}, u \in \mathbf{U}, \tag{1}$$

where p_{iu}^t is the transmit power from node i to node u. The random variable g_{iu} accounting for multipath fading follows an exponential distribution with mean $\frac{1}{\mu}$. $d_{iu} = \sqrt{|x_i - x_u|^2 + |y_i - y_u|^2}$ is the distance between node i and node u, where (x_i, y_i) and (x_u, y_u) denote locations of node i and node u in the Voronoi tessellation. Path loss exponent is α.

3.1. Primary and Secondary Cell Association

Cross-carrier scheduling maximizes the transmission quality by aggregating the control signals of multiple carriers into a single control channel, which makes individual UE

experience less interference from neighbor cells [3]. The CC with the highest quality signal among all the aggregated CCs serves as PCC for transmissions of control signals and data, while the remaining aggregated CCs serve as SCCs only for data transmission. Then, the SCCs can be dynamically activated without unnecessary control channel interference in densely deployed cellular networks by arranging the control signals to PCC [3]. In this paper, we assume that, within the coverage area of each CC, RBs for users with same type of APs are uniformly allocated, which turns the RB resource allocation problem into a UE aggregation problem for each CC.

The CCs aggregated and utilized by AP i to communicate with serving UE, which are aggregated in Voronoi cell V_i, are shown as [28]

$$\mathbf{U}_i \stackrel{\text{def}}{=} \cup\{u_i : u \in \mathbf{U} \cap V_i\}, \tag{2}$$

where the $\mathbf{U}_i$ is the set of UE associated with the AP i.

To analyze the characteristics of UE aggregation for each AP, we introduce a non-negative function $f(u)$ defined on $\mathbf{R}^2$, which is shown as [29]

$$f(u_i) = \sum_{u \in \mathbf{U}} f(u)\mathbf{1}\{u \in V_i\}. \tag{3}$$

where $\mathbf{1}$ is the identify function between AP i and UE u and shown as

$$\mathbf{1} = \begin{cases} 1, & \text{if } u \in V_i, \\ 0, & \text{otherwise.} \end{cases} \tag{4}$$

Then,

$$E\{f(u_i)\} = \lambda_u E\{\int f(u)\mathbf{1}\{u \in V_i\}\}. \tag{5}$$

Conditions that one CC can be utilized by AP i for communicating with UE u are shown as follows [18]:

$$\{u \in V_i\} \stackrel{\text{def}}{=} \{N^I = 0, N^J = 0, d_{ju} > (\frac{\psi_u p_{iu}^t}{p_{ju}^t})^{-\alpha^{-1}} d_{iu}\}, \tag{6}$$

where V_i is the Voronoi cell for AP i. N^I and N^J are the numbers of APs from AP sets I and J utilizing the same CC in the coverage centered in u with radius d_{iu} and d_{ju}, respectively, i.e., $I, J \in \{S, W\}$ and $I \neq J$.

In (6), one CC is aggregated by AP i to communicate with UE $u \in \mathbf{U}$ if and only if the following conditions are satisfied:

① There are no APs from set **I** utilizing the same CC in the coverage that centered in u with radius d_{iu}.

② There are no APs from set **J** utilizing the same CC in the coverage that centered in u with radius d_{ju}.

③ AP j shows more disadvantage than AP i with bias parameter $(\frac{\psi_u p_{iu}^t}{p_{ju}^t})^{-\alpha^{-1}}$.

In the perspective of distance, the conditions shown above are that the serving AP i is the nearest AP among all the APs in set **I** utilizing the same CC at a distance d_{iu} to UE u and shows advantage in distance over the nearest AP j from set **J** utilizing the same CC at a distance d_{ju} to UE u with bias parameter $(\frac{\psi_u p_{iu}^t}{p_{ju}^t})^{-\alpha^{-1}}$. Then, the CC is aggregated by the AP i and utilized in the communication with UE u.

It is worthwhile to mention that the delay-sensitive UE associated with small-cell APs can utilize 5G and 5G-U, while the rate-sensitive UE associated with Wi-Fi APs can only utilize unlicensed spectra, which means there are no conditions ① and ② when it comes to 5G licensed band.

Then, the null probability of d_{iu} is shown as follows [28]:

$$Pr\{u \in \mathbf{V}_i\} = e^{-(\lambda_I \pi {d_{iu}}^2 + \lambda_J \pi \{(\frac{\psi_u p_{iu}^t}{p_{ju}^t})^{-\alpha^{-1}} d_{iu}\}^2)}, \tag{7}$$

where λ_I and λ_J are densities of APs aggregating the same CC from I and J, respectively. d_{iu} and d_{ju} are the distances between UE u and the closest APs utilizing same CC from I and J, respectively. Then, the cumulative distribution function (CDF) of d_{iu} is [30]

$$Pr\{d_{ju} \leq (\frac{\psi_u p_{iu}^t}{p_{ju}^t})^{-\alpha^{-1}} d_{iu}\} = 1 - e^{-\phi \pi {d_{iu}}^2}, \tag{8}$$

where $\phi = (\lambda_I + \lambda_J (\frac{\psi_u p_{iu}^t}{p_{ju}^t})^{-2\alpha^{-1}})$. And the probability density function (PDF) of d_{iu} can be found as

$$f_r(r) = e^{-\phi \pi r^2} 2\pi\phi r, \tag{9}$$

with random value r replacing d_{iu}.

3.2. Outage Probability

The outage probability of a randomly located UE at distance r with the tagged AP is shown as follows [28]:

$$\begin{aligned} Pr_i^o(\lambda_I, \lambda_J, \beta, \alpha) &= E_r[Pr[SINR \leq \beta | r]] \\ &= 1 - E_r[Pr[SINR > \beta | r]] \\ &= 1 - \int_{r>0} Pr[\frac{p_{iu}^t g r^{-\alpha}}{\mathbf{Ic}_i + \sigma^2} > \beta | r] f_r(r) dr \\ &= 1 - \int_{r>0} Pr[g > \beta {p_{iu}^t}^{-1} r^\alpha (\mathbf{Ic}_i + \sigma^2) | r] f_r(r) dr, \end{aligned} \tag{10}$$

where β is the threshold for the received signal-to-interference-plus-noise ratio $(SINR)$. $\mathbf{Ic}_i$ and σ^2 are co-channel interference power set and white Gaussian noise, respectively.

With the fact that $g \sim exp(\mu)$ [31], we can obtain

$$\begin{aligned} Pr[g > \beta {p_{iu}^t}^{-1} r^\alpha (\mathbf{Ic}_i + \sigma^2) | r] &= E_{\mathbf{Ic}_i}[Pr[g > \beta {p_{iu}^t}^{-1} r^\alpha (\mathbf{Ic}_i + \sigma^2) | r, \mathbf{Ic}_i]] \\ &= e^{-\mu\beta {p_{iu}^t}^{-1} r^\alpha \sigma^2} L_{\mathbf{Ic}_i}(\mu\beta {p_{iu}^t}^{-1} r^\alpha) \end{aligned} \tag{11}$$

and

$$\begin{aligned} L_{\mathbf{Ic}_i}(\mu\beta {p_{iu}^t}^{-1} r^\alpha) &= E_{\mathbf{\Phi},g}[\prod_{i \in \mathbf{\Phi}} E_g[exp(\mu\beta {p_{iu}^t}^{-1} r^\alpha)]] \\ &= E_{\mathbf{\Phi},g}[\prod_{i \in \mathbf{\Phi}} \int exp(\mu\beta {p_{iu}^t}^{-1} r^\alpha) \mu exp(-\mu g) d_g] \\ &= E_{\mathbf{\Phi}}[\prod_{i \in \mathbf{\Phi}} \frac{1}{1 + \beta {p_{iu}^t}^{-1} r^\alpha v^{-\alpha}}] \\ &= exp(-2\pi\phi \int_r^\infty \frac{\beta}{\beta + (\frac{v}{r})^\alpha} v dv) \end{aligned} \tag{12}$$

with $r^2 \to v$ and $\mathbf{\Phi}$ is the interference set for the downlink communication between AP i and UE u.

3.3. Reserved Unlicensed Spectrum Minimization Problem with QoS Satisfying Rate-Sensitive UE

Due to the CSMA/CA feature of UE in the Wi-Fi system, small-cell UE in 5G-U can take over an unlicensed spectrum and cause degradation regarding the performance of the

Wi-Fi system, which can be overcome by reserving a partial unlicensed spectrum for the Wi-Fi system [6]. To guarantee the performance of rate-sensitive UE associated with Wi-Fi APs, a portion of unlicensed spectrum needs to be saved, which also guarantees the PCC for rate-sensitive UE.

The mean ergodic achievable rate C_w for UE u in the downlink communication from any Wi-Fi AP $w \in W$ on condition that the tagged AP is at a distance r from the UE is shown as follows [28]:

$$C_w(b_w, p_w^t) = \int_{r>0} e^{-\phi\pi r^2} \omega 2\pi\phi r dr, \tag{13}$$

where

$$\omega = \int_{t>0} e^{-\mu {p_w^t}^{-1} r^\alpha \sigma^2 (2^{\frac{1}{b_w t}} - 1)} L_{\mathbf{Ic}_w}(\mu {p_w^t}^{-1} r^\alpha (2^{\frac{1}{b_w t}} - 1)) dt \tag{14}$$

with b_w and p_w^t as virtual carrier bandwidth and transmit power for Wi-Fi AP to UE and

$$L_{\mathbf{Ic}_w}(\mu {p_w^t}^{-1} r^\alpha (2^{\frac{1}{b_w t}} - 1)) = exp(-2\pi\phi \int_r^\infty (1 - \frac{1}{1 + {p_w^t}^{-1} (\frac{r}{v})^\alpha (2^{\frac{1}{b_w t}} - 1)}) v dv). \tag{15}$$

In the Poisson–Voronoi (PV) system, mean average length of connections from Wi-Fi AP to UE, which is also the radius of Wi-Fi cell coverage, is obtained according to Voronoi properties as follows [29]:

$$E[l_w] = \frac{E[L_u^w]}{E[N_u^w]} = \frac{\frac{\delta_u}{2{\delta_w}^{\frac{3}{2}}}}{\frac{\delta_u}{\delta_w}} = \frac{1}{2{\delta_w}^{\frac{1}{2}}}, \tag{16}$$

where $E[N_u^w]$ and $E[L_u^w]$ are the mean number of UE in one Wi-Fi cell coverage and the mean total length of connections from Wi-Fi AP to UE, respectively.

The mean number of UE in one Wi-Fi cell coverage is given as [32]

$$E[N_u^w] = \delta_u 2\pi \int_0^\infty l_w e^{-\delta_w \pi l_w^2} dl_w = \frac{\delta_u}{\delta_w}, \tag{17}$$

where l_w represents the radius of Wi-Fi cell coverage. By utilizing the same method, the mean number of UE in one small cell coverage is $E[N_u^s] = \frac{\delta_u}{\delta_s}$.

With slight modifications in (17), the mean total length of connections from Wi-Fi AP to UE can be shown as follows:

$$E[L_u^w] = \delta_u 2\pi \int_0^\infty l_w^2 e^{-\delta_w \pi l_w^2} dl_w = \frac{\delta_u}{2{\delta_w}^{\frac{3}{2}}}, \tag{18}$$

and mean total length of connections from small cell AP to UE $E[L_u^s] = \frac{\delta_u}{2{\delta_s}^{\frac{3}{2}}}$.

With the Voronoi properties mentioned above, the mean average length of connections from Wi-Fi AP to UE, which can also be interpreted as the radius of Wi-Fi cell coverage, is obtained as

$$E[l_w] = \frac{E[L_u^w]}{E[N_u^w]} = \frac{\frac{\delta_u}{2{\delta_w}^{\frac{3}{2}}}}{\frac{\delta_u}{\delta_w}} = \frac{1}{2{\delta_w}^{\frac{1}{2}}}. \tag{19}$$

As mentioned above, if we uniformly allocate aggregated RBs to Wi-Fi APs and each virtual carrier in downlink communication behavior, then $b_w = \frac{(1-\gamma)B}{Ar\delta_u}$, where γ is the ratio of unlicensed spectrum allocated to small-cell APs in area Ar. By applying the same method, $p_w^t = \frac{\xi P}{Ar\delta_u}$, in which ξ is the ratio of power allocated to Wi-Fi APs. B and P are the total unlicensed spectrum and power, respectively.

To protect the performance of rate-sensitive UE associated with Wi-Fi APs, we set a Wi-Fi system performance guard threshold to guarantee that the mean achievable rate for rate-sensitive UE associated with Wi-Fi APs is no less than C_t. Then, the pre-reserved unlicensed spectrum minimization problem **P1** for rate-sensitive UE is proposed to achieve the minimum unlicensed spectrum to protect the network performance of Wi-Fi users, as shown in (20).

$$\begin{aligned} \mathbf{P1}: \min_{\gamma,\xi} \quad & \sum b_w(\gamma,\xi) \\ \text{s.t.} \quad & \sum b_w \le B, w \in \mathbf{W} \\ & E[C_w](\gamma,\xi) \ge C_t, w \in \mathbf{W} \\ & Pr_w^c \le Pr_{thr,w}^c, w \in \mathbf{W} \end{aligned} \tag{20}$$

where the summation of unlicensed band used by the Wi-Fi users should not be greater than the provided system spectrum bandwidth B. The mean achievable rate for rate-sensitive UE associated with Wi-Fi APs is $E[C_w]$. The Pr_w^o and $Pr_{thr,w}^o$ are the outage probability and outage probability threshold for rate-sensitive UE associated with Wi-Fi APs, respectively. The pre-reserved unlicensed spectrum minimization problem for rate-sensitive UE can be solved by utilizing the Gradient descent method with the Bisection method [33].

Numerical results for the optimization problem (20) are shown in Figure 2, which represents the mean achievable rate of rate-sensitive UE $E[C_w]$ as a function of unlicensed spectrum allocation ratio γ with different power ratios ξ. In Figure 2, with γ increasing from 0.05 to 0.95 when the power ratio is 0.5, $E[C_w]$ decreases due to the decrease in the allocated unlicensed spectrum. With power allocation ratio ξ increasing, $E[C_w]$ increases in the same spectrum allocation ratio. Specifically, with ξ increasing, optimal γ for maximum $E[C_w]$ increases due to inter-channel interference between UE. The QoS threshold of the Wi-Fi system shown in the figure guarantees the performance of rate-sensitive UE by restricting the maximum unlicensed spectrum allocation ratio γ for the corresponding power allocation ratio ξ, which also implies that the minimum spectrum resources need to be served to guarantee the performance of rate-sensitive UE associated with Wi-Fi APs.

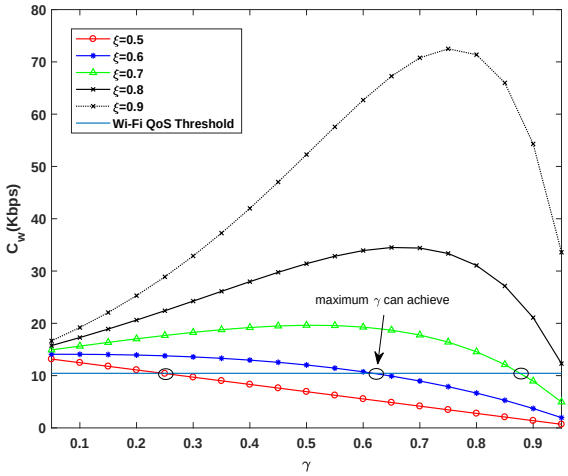


Figure 2. Mean ergodic achievable rate for rate-sensitive UE as a function of γ with Wi-Fi system performance threshold.

3.4. Mean Packet Transmission Delay for Delay-Sensitive UE QoS Requirement

We model one M/G/1 queue in each AP for downlink communications to analyze the time-domain behaviors of delay-sensitive UE; then, the mean packet transmission delay in small-cell AP, $E[D_s|b_s, p_s^t]$, is shown as [18]

$$E[D_s|b_s, p_s^t] = E[S_s|b_s, p_s^t] + E[W_s|b_s, p_s^t], \tag{21}$$

where $E[S_s|b_s, p_s^t]$ is the mean service time. The mean waiting time for packets in the AP $E[W_s|b_s, p_s^t]$ with given b_s and p_s^t is shown as [34]

$$E[W_s|b_s, p_s^t] = E[L_s]E[S_s|b_s, p_s^t] + \rho_s E[R_s|b_s, p_s^t], \tag{22}$$

where $E[L_s]$ denotes the number of packets in small-cell APs and $\rho_s = \lambda_s E[S_s]$ is the utility ratio. $E[S_s|b_s, p_s^t]$ and $E[R_s|b_s, p_s^t]$ are mean service time and residual service time, respectively. $\rho_s = \lambda_s E[S_s]$ is the utility ratio and, in order to ensure the stability of the queue system, condition $\rho_s \leq 1$ must be satisfied.

With the Little's law and relationship between service time and residual service time [34], $E[R_s|b_s, p_s^t] = E[S_s^2|b_s, p_s^t]/2E[S_s|b_s, p_s^t]$, mean waiting time in (22) can also be represented as

$$E[W_s|b_s, p_s^t] = \frac{\rho_s E[S_s^2|b_s, p_s^t]}{2(1-\rho_s)E[S_s|b_s, p_s^t]}. \tag{23}$$

Therefore, the mean packet transmission delay in small-cell AP, $E[D_s|b_s, p_s^t]$, is shown as [18]

$$E[D_s|b_s, p_s^t] = E[S_s|b_s, p_s^t] + \frac{\rho_s E[S_s^2|b_s, p_s^t]}{2(1-\rho_s)E[S_s|b_s, p_s^t]}. \tag{24}$$

We define service time S_s as packet transmission processing time in the AP, which means $E[S_s] = 1/C_s$ per unit-length packet. Then, the CDF of S_s can be obtained as

$$F_{S_s}(t|b_s, p_s^t) = Pr[g > \frac{(2^{\frac{1}{b_s t}} - 1)(\mathbf{Ic_s} + \sigma^2)}{p_s^t r^{-\alpha}}]. \tag{25}$$

With the fact that $g \sim exp(h)$ [27], we can obtain

$$Pr[g > \frac{(2^{\frac{1}{b_s t}} - 1)(\mathbf{Ic_s} + \sigma^2)}{p_s^t r^{-\alpha}}] = e^{-h\frac{(2^{\frac{1}{b_s t}}-1)\sigma^2}{p_s^t r^{-\alpha}}} L_{\mathbf{Ic}_s}(h\frac{(2^{\frac{1}{b_s t}} - 1)}{p_s^t r^{-\alpha}}), \tag{26}$$

and

$$L_{\mathbf{Ic}_s}(h\frac{(2^{\frac{1}{b_s t}} - 1)}{p_s^t r^{-\alpha}}) = exp(-2\pi\phi \int_r^\infty \frac{\frac{(2^{\frac{1}{b_s t}}-1)}{p_s^t}}{\frac{(2^{\frac{1}{b_s t}}-1)}{p_s^t} + (\frac{\tau}{r})^\alpha} \tau d\tau). \tag{27}$$

Then, the PDF of the service time, S_s, can be given as

$$f_{S_s}(t|b_s, p_s^t) = (e^{-h\frac{(2^{\frac{1}{b_s t}}-1)\sigma^2}{p_s^t r^{-\alpha}}})' L_{\mathbf{Ic}_s}(h\frac{(2^{\frac{1}{b_s t}} - 1)}{p_s^t r^{-\alpha}}) + e^{-h\frac{(2^{\frac{1}{b_s t}}-1)\sigma^2}{p_s^t r^{-\alpha}}} L'_{\mathbf{Ic}_s}(h\frac{(2^{\frac{1}{b_s t}} - 1)}{p_s^t r^{-\alpha}}) \tag{28}$$

where $(e^{-h\frac{(2^{\frac{1}{b_s t}}-1)\sigma^2}{p_s^t r^{-\alpha}}})'$ and $L'_{\mathbf{Ic}_s}(h\frac{(2^{\frac{1}{b_s t}} - 1)}{p_s^t r^{-\alpha}})$ can be achieved by differentiation operations. With conditional PDF of the service time, we can obtain the mean packet transmission delay in small-cell APs.

The mean packet transmission delay minimization problem **P2** for the delay-sensitive UE with objective function and constraints is given in (29).

$$\begin{aligned} \mathbf{P2}: \min_{\gamma,\xi} \quad & E[D_t](\gamma,\xi) \\ \text{s.t.} \quad & \sum_{i=1}^{I} b_i = B, \quad i \in \{1,\ldots,I\}, \\ & \sum_{i=1}^{I} p_i = P, \quad i \in \{1,\ldots,I\}, \\ & \rho_i \leq 1, \quad i \in \{1,\ldots,I\}, \\ & 0 \leq \gamma, \xi \leq 1, \end{aligned} \tag{29}$$

where b_i and p_i are the spectrum bandwidth and power allocated to delay-sensitive UE i with $i \in \{1,\ldots,I\}$. The optimization problem can also be solved by utilizing the Gradient descent method with the Bisection method.

Figure 3 shows the mean packet transmission delay for delay-sensitive UE as a function of unlicensed spectrum allocation ratio γ with each power allocation ratio ξ. The QoS threshold of small-cell APs shown in Figure 3 guarantees the performance of delay-sensitive UE by restricting the minimum unlicensed spectrum allocation ratio γ for the corresponding power allocation ratio ξ. In the figure, to provide the consistent mean packet transmission delay for delay-sensitive UE, more spectrum resource is needed for a smaller power allocation ratio to delay-sensitive UE, and vice versa.

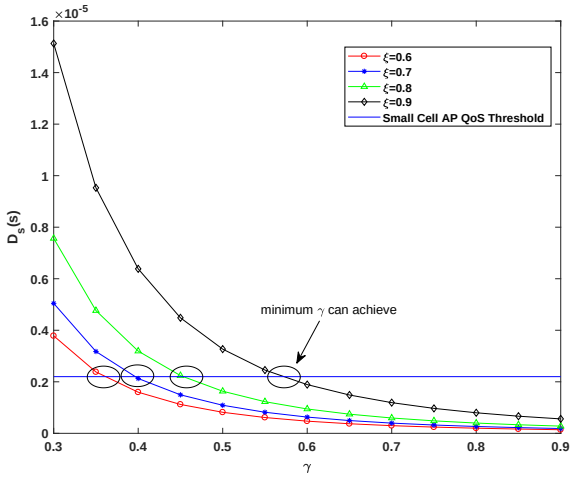


Figure 3. Packet transmission delay for delay-sensitive UE as a function of unlicensed spectrum allocation ratio γ.

Figure 4 shows the mean packet transmission delay for rate-sensitive UE as a function of unlicensed spectrum allocation ratio γ for various power allocation ratios ξ, respectively. As the figure shows, rate-sensitive UE is not sensitive to the change in packet transmission delay as the allocations of power and spectrum resources change, until the γ is over 0.75 due to the reserved spectrum resource.

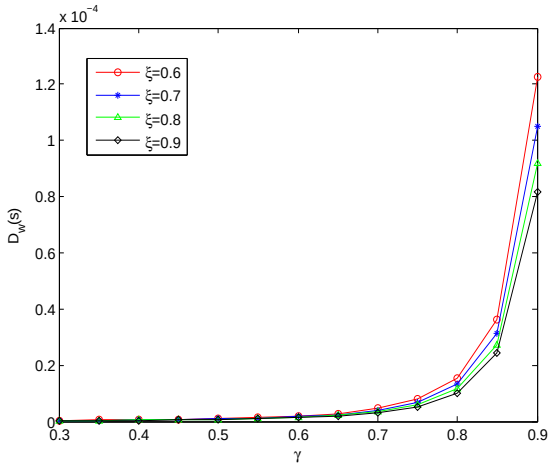


Figure 4. Packet transmission delay for rate-sensitive UE as a function of unlicensed spectrum allocation ratio γ.

Figure 5 shows total packet transmission delay for all UE in the network as a function of unlicensed spectrum allocation ratio γ for various power allocation ratios ξ. It shows that the total packet transmission delay has the same variation tendency as the packet transmission delay for rate-sensitive UE, as shown in Figure 4, which means that the total packet transmission delay is mainly caused by the rate-sensitive UE in the system. Then, this reveals that it is essential to choose the most accurate performance criteria for the UE in the system.

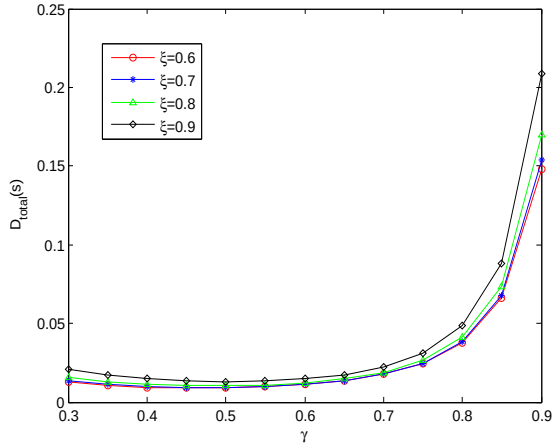


Figure 5. Total packet transmission delay as a function of unlicensed spectrum allocation ratio γ.

Then, all in range CCs of the UE u are arranged based on their signal qualities. The CC offering the highest signal quality in 5G receives an assignment of identify function with 1 for the PCC by the UE u, and the remaining CCs in both 5G and 5G-U can also receive identify function with 1 for SCCs based on the association mechanism.

The delay-sensitive UE and rate-sensitive UE have a minimum QoS requirement on delay and rate, which are D_{max} and c_{min}, respectively. Then, an association bias ψ can be achieved based on the proportional fairness of each UE in the network. From the perspective of APs, each AP allocates resources to UE in its cell coverage with the highest association bias ψ, which is shown as

$$\psi = \frac{Minimum\ QoS\ Requirement}{Real\ Time\ QoS}. \tag{30}$$

The procedure of dynamic unlicensed spectrum allocation is presented in Algorithm 1.

Algorithm 1: Proposed algorithm for primary and secondary CCs association

Algorithm input: All in range CCs in 5G and 5G-U.
Initialize Primary and secondary CCs allocation.
begin
  Identify function to the AP serving highest signal quality ← 1;
  if *The AP also assign an identify function with* 1 *to UE u* **then**
    aggregation set ← CC;
    Break;
  else
    Remove AP from the list and return to **Step 3**;
  end if
end
Algorithm output: PCC and SCCs.

With this dynamic primary and secondary CCs association mechanism, UE in the network can be optimally allocated primary and secondary CCs by considering proportional fairness based on carrier quality and service type. A simple flowchart representing the process of this work is shown in Figure 6.

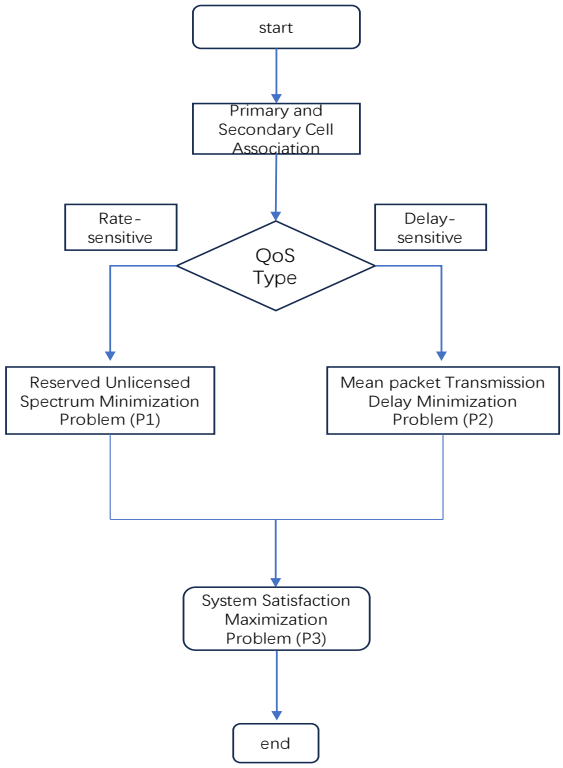


Figure 6. The flowchart of resource allocation process for 5G network under unlicensed band with CA feature.

4. Problem Formulation

System Satisfaction Maximization Problem

In the Poisson–Voronoi (PV) system, the expected number of UE in one small-cell coverage is given as [29]

$$E[N_u^s] = \delta_u 2\pi \int_0^\infty l_s e^{-\delta_s \pi l_s^2} dl_s = \frac{\delta_u}{\delta_s}, \tag{31}$$

where l_s represents the radius of the small-cell coverage. With the same procedure, the expected number of UE in one Wi-Fi cell coverage $E[N_u^w] = \frac{\delta_u}{\delta_w}$.

With slight modifications in (31), the expected numbers of small-cell APs and Wi-Fi APs in one MBS cell coverage are $\frac{\delta_s}{\delta_m}$ and $\frac{\delta_w}{\delta_m}$, respectively.

The Jain fairness index (JFI) has been used significantly in the fairness criterion literature for resource allocation [17]. Jain's fairness index is

$$f(x) = \frac{(\sum_{i=1}^{N} x_i)^2}{N \sum_{i=1}^{N} x_i^2}, \tag{32}$$

where N denotes the total number of users and x_i denotes the received allocation for the i_{th} user.

Based on Jain's fairness index, the fairness index when considering UE's QoS requirements is defined so as to maximize the UE satisfaction valuation. Then, in this section, we consider system utility function based on the satisfaction degree of each UE to the QoS provided by the system, which is defined as the ratio of QoS to system performance threshold. To balance the desperate desire of network operators to provide better network service for delay-sensitive UE and promised network performance for rate-sensitive UE, we consider the weight factor η between system satisfaction of delay-sensitive UE and rate-sensitive UE.

The objective of the system is to maximize the overall UE satisfaction, shown as

$$\begin{aligned} \textbf{P3:} \max_{\gamma,\xi,\eta} \quad & \eta \sum_{w=1}^{W} \frac{C_w}{C_t} - (1-\eta) \sum_{s=1}^{S} \frac{D_s}{D_t} \\ \text{s.t.} \quad & b_w \geq b_w^*, w \in \mathbf{W} \\ & E[D_s](\gamma,\xi,\eta) \leq D_t^*, s \in \mathbf{S} \\ & Pr_s^c \geq Pr_{thr,s}^c, s \in \mathbf{S} \\ & 0 \leq \gamma, \xi, \eta \leq 1, \\ & \rho_s \leq 1, s \in \mathbf{S} \end{aligned} \tag{33}$$

where b_w^* and D_t^* are the solutions achieved in the optimization problem **P1** and **P2**, which are considered as the performance threshold to guarantee the mean achievable rate and mean packet delay for rate-sensitive and delay-sensitive UE. The minus sign for delay-sensitive UE is due to the fact that delay is preferred to be minimized in the maximization problem.

The procedure of system satisfaction maximization via optimal resource allocation by utilizing the Gradient descent method with the Bisection method [33] for 5G under unlicensed band with CA is presented in Algorithm 2.

Algorithm 2: System Satisfaction Maximization Algorithm

Algorithm input: $\mathbf{G}(\{\mathbf{M}, \mathbf{S}, \mathbf{W}\}, \mathbf{U})$, δ_m, δ_s, δ_w, δ_u, Step size θ, tolerance $\epsilon > 0$.
Initialize γ, ξ with $\rho_s(\gamma, \xi) \leq 1$ and $0 \leq \gamma, \xi \leq 1$
begin
  Obtain b_w from (29).
  if $\sum b_w = B$ **then**
    Stop;
  else
    $b_w^1 = \sum b_w$;
    Achieve maximum system satisfaction from (33) and the corresponding b_w by utilizing Gradient descent method with step size θ;
    $b_w^2 = \sum b_w$;
    $b_w^* = max\{b_w^1, \ldots, b_w^I\}$.
    $\gamma^* = 1 - \frac{b_w^*}{B}$.
    if $||\nabla \sum_{i=1}^{I} E[D_i](\xi|\gamma^*)||_2 \leq \epsilon$, **then**
      $\xi^* = \xi$;
      Break;
    else
      Update ξ by using Bisection method and return to **Step 3**;
    end if
  end if
end
Algorithm output: $\gamma*$, $\xi*$ (Optimal unlicensed spectrum and power allocation ratio).

5. Numerical Results

We investigate a 5G network under an unlicensed band with a CA feature within one MBS cell coverage with dimensions 1 km × 1 km × 1 km. The parameters for simulation are summarized in Table 2.

Table 2. Simulation parameters.

Definition	Value
δ_m	$1/\text{km}^2$
δ_s	$1000/\text{km}^2$
δ_w	$1000/\text{km}^2$
δ_u	$10{,}000/\text{km}^2$
Total spectrum	1000 MHz
Total power	100 mW
Step size θ	0.05

Figure 7 shows the comparison between the peak data rate for rate-sensitive UE with a CA feature and that without a CA feature, which results in superior performance in improving mean achievable peak data rate for rate-sensitive UE. In the figure, the peak data rate for rate-sensitive UE with a CA feature keeps increasing as ξ increases. Meanwhile, the peak data rate reaches the maximum point as γ reaches the optimal value γ^*, and then decreases as γ keeps increasing due to the shortage of spectrum resource to match the allocated power resource.

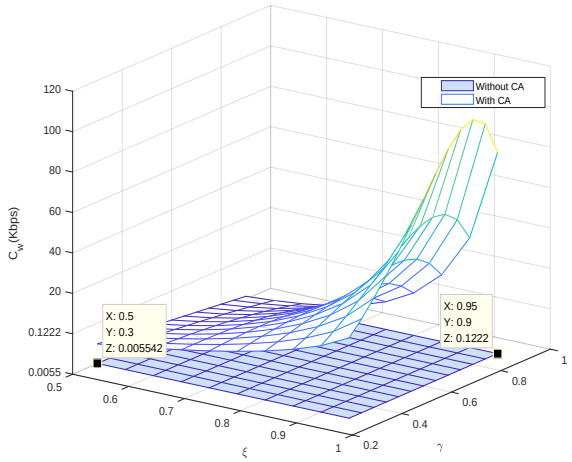


Figure 7. Comparison of peak data rate for rate-sensitive UE with CA and without CA.

Figure 8 shows the comparison between mean packet transmission delay for delay-sensitive UE with a CA feature and that without a CA feature, which results in superior performance in decreasing mean packet transmission delay for delay-sensitive UE. η is 0.5 in Figures 7 and 8. In the figure, the mean packet transmission delay for delay-sensitive UE with a CA feature reaches the minimum value as the γ is the maximum and the ξ is the minimum. In the figure, the variation tendency of mean packet transmission delay is faster with the change in γ as compared to that of ξ, which means that the delay-sensitive UE is more sensitive to the spectrum resource.

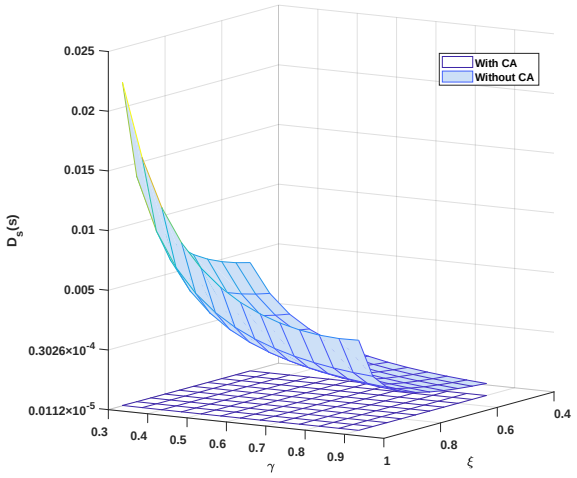


Figure 8. Comparison of packet transmission delay for delay-sensitive UE with CA and without CA.

Figure 9 shows system satisfaction as a function of unlicensed spectrum allocation ratios γ for various power allocation ratio ξ. The value of system satisfaction reaches its maximum when γ is optimal and the value of optimal γ increases with the power allocation ratio ξ increasing. Also, the value of system satisfaction drops rapidly after the γ reaches the optimal point due to the influence on the rate-sensitive UE. The value of system satisfaction increases as ξ increases due to the rate-sensitive UE being more sensitive to power allocation. As shown in the figure, the proposed scheme achieves superior system satisfaction with ξ^* as compared to that when ξ is other values achieved by utilizing the Monte Carlo simulation.

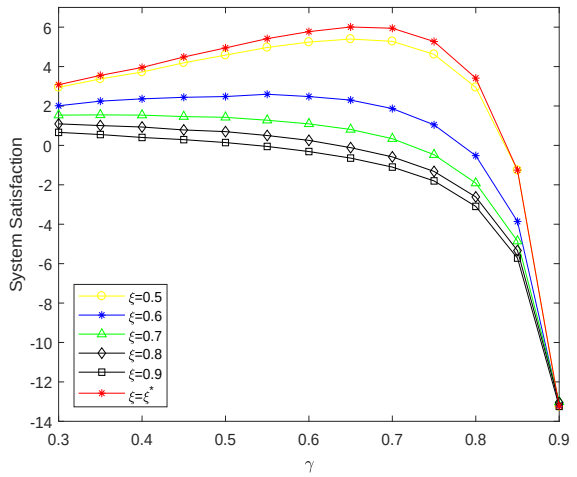


Figure 9. System satisfaction as a function of unlicensed spectrum allocation ratio γ.

Figure 10 shows system satisfaction in Figure 9 as a function of power allocation ratio ξ for various unlicensed spectrum allocation ratios γ. This shows that the optimal value of spectrum allocation ratio ξ for the maximum system satisfaction keeps changing as the power allocation ratio ξ increases. When the ξ is small, the corresponding γ with the smallest value contributes to the maximum system satisfaction since the rate-sensitive UE needs more spectrum resources to compensate for the shortness of power resource. As the power resource allocation ratio ξ increases, the optimal value of γ for the maximum system satisfaction decreases, which is due to the optimal point of γ, as shown in Figure 9. As shown in the figure, the proposed scheme achieves superior system satisfaction with γ^* than that when γ is other values achieved by utilizing the Monte Carlo simulation.

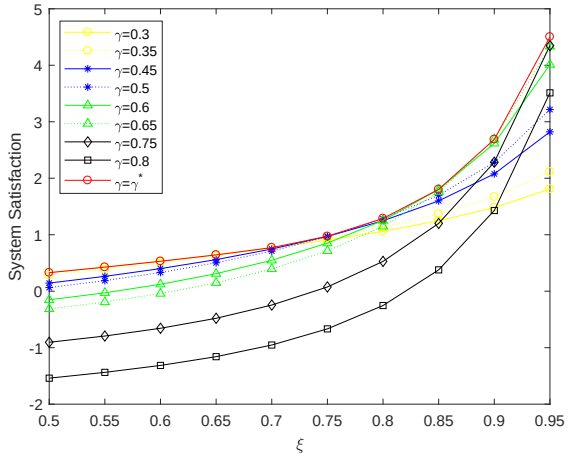


Figure 10. System satisfaction as a function of power allocation ratio ξ.

Figure 11 shows the optimal unlicensed spectrum allocation ratio γ and power allocation ratio ξ for maximum system satisfaction, as shown in the Figures 9 and 10 in the third dimension in the figure when η is 0.5. In the figure, the optimal value of γ, γ^*, increases as ξ increases to match with each for the maximum system satisfaction, which also results in the maximum resource usage efficiency. Meanwhile, the optimal value of ξ, ξ^*, remains consistent until the γ reaches a certain point, which means that the rate-sensitive UE is more sensitive to power allocation with the reserved spectrum resource. The maximum system satisfaction shows better performance with larger η, as shown in the figure, which means that the performance of rate-sensitive UE is efficiently protected with the proposed scheme. To demonstrate the effectiveness of the proposed scheme, we present a performance comparison of the proposed scheme with that throughput as the only network performance metric considered in the system.As shown in the figure, the proposed mechanism achieves superior maximum system satisfaction and γ^* and ξ^* are achievable compared with the scheme in which only throughput is considered as a QoS metric in the system, which is widely used by the related works, as shown in Section 2 of this paper.

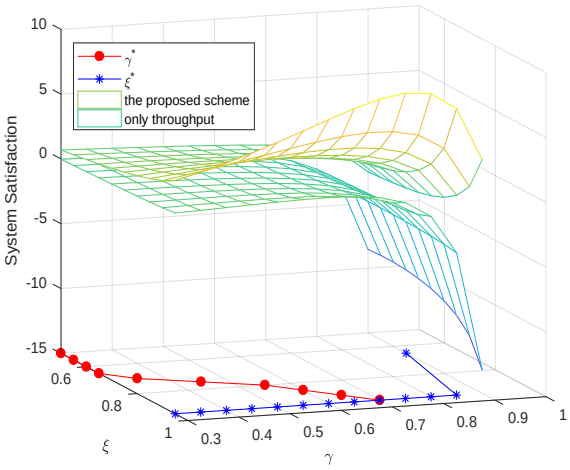


Figure 11. The optimal γ and ξ for maximum system satisfaction in 3D with performance comparison for the proposed scheme.

6. Conclusions

In this paper, we proposed an optimal resource allocation mechanism to maximize the system satisfaction for two types of UEs with different QoS requirements in the 5G network under an unlicensed band with CA technology. To overcome the main challenge of the 5G-U network, the minimum unlicensed spectrum was firstly reserved to guarantee the performance of rate-sensitive UE in the unlicensed band. By utilizing the M/G/1 queue

model, the mean packet transmission delay for delay-sensitive UE is achieved, which restricted the minimum unlicensed spectrum to satisfy the QoS requirement for delay-sensitive UE. With the minimum QoS requirement for each type of UE, a system satisfaction maximization problem with an optimal association bias was formulated by considering the fairness index for each UE to optimize the overall network performance. Then, the optimal unlicensed spectrum and power allocation ratio can be obtained by maximizing the system satisfaction under the derived constraints. The numerical results demonstrate that the proposed mechanism achieved the maximum system satisfaction effectively by considering the network performance bias between the rate-sensitive and delay-sensitive data. The designed mechanism efficiently protected the system performance of Wi-Fi UE, which demonstrated that the CA technology can be the solution for the 5G-U network. Meanwhile, the CA technology successfully empowered the 5G-U network considering multiple performance metrics. Lastly, the optimal resource allocation maximized the system satisfaction, which proved to be superior than the widely used scheme in which only throughput is considered. Based on the achievements gained from this paper, in future studies, we will consider the system with a non-uniform allocation of resources among APs belonging to the same QoS service type.

Author Contributions: Conceptualization, J.L.; methodology, J.L. and T.Z.; software, W.G.; validation, X.L.; formal analysis, J.L. and W.G.; investigation, X.L.; resources, J.L.; data curation, T.Z.; writing—original draft preparation, J.L.; writing—review and editing, T.Z.; visualization, W.G.; supervision, X.L.; project administration, X.L.; funding acquisition, J.L. All authors have read and agreed to the published version of the manuscript.

Funding: This work was an R&D Program of Beijing Municipal Education Commission (KM202310011002).

Institutional Review Board Statement: Not applicable.

Informed Consent Statement: Not applicable.

Data Availability Statement: The data that support the findings of this study are available from the corresponding author upon reasonable request.

Conflicts of Interest: The authors declare no conflict of interest.

References

1. Bajracharya, R.; Shrestha, R.; Jung, H. Future Is Unlicensed: Private 5G Unlicensed Network for Connecting Industries of Future. *Sensors* **2020**, *20*, 2774. [CrossRef] [PubMed]
2. Adamu, P.U.; Lopez-Benitez, M. Performance evaluation of carrier aggregation as a diversity technique in mmWave bands. In Proceedings of the IEEE VTC2021-Spring, Helsinki, Finland, 25–28 April 2021.
3. Wang, C.Y.; Wei, H.Y.; Chen, W.T. Resource block allocation with carrier-aggregation: A strategy-proof auction design. *IEEE Trans. Mob. Comput.* **2016**, *15*, 3142–3155. [CrossRef]
4. Zhang, H.; Chu, X.; Guo, W.; Wang, S. Coexistence of Wi-Fi and heterogeneous small cell networks sharing unlicensed spectrum. *IEEE Commun. Mag.* **2015**, *53*, 158–164. [CrossRef]
5. AI-Dulaimi, A.; AI-Rubaye, S.; Ni, Q.; Sousa, E. 5G Communications Race: Pursuit of More Capacity Triggers LTE in Unlicensed Band. *IEEE Veh. Technol. Mag.* **2015**, *10*, 43–51. [CrossRef]
6. Naik, G.; Park, J.; Ashdown, J.; Lehr, W. Next Generation Wi-Fi and 5G NR-U in the 6 GHz Bands: Opportunities and Challenges. *IEEE Access* **2020**, *8*, 153027–153056. [CrossRef]
7. Lee, J.; Yi, Y.; Chong, S.; Jin, Y. Economics of WiFi offloading: Trading delay for cellular capacity. *IEEE Trans. Wirel. Commun.* **2014**, *13*, 1540–1554. [CrossRef]
8. Bao, H.; Huo, Y.; Dong, X.; Huang, C. Joint time and power allocation for 5G NR unlicensed systems. *IEEE Trans. Wirel. Commun.* **2021**, *19*, 6195–6209. [CrossRef]
9. Zhou, Z.; Teng, F.; Liu, J.; Xiao, W. Performance evaluation for coexistence of LTE and WiFi. In Proceedings of the International Conference on Computing, Networking and Communications (ICNC), Kauai, HI, USA, 15–18 February 2016.
10. Cavalcante, A.M.; Almeida, E.; Vieira, R.D.; Choudhury, S.; Tuomaala, E.; Doppler, K.; Chaves, F.; Paiva, R.C.D.; Abinader, F. Performance Evaluation of LTE and Wi-Fi Coexistence in Unlicensed Bands. In Proceedings of the IEEE 77th Vehicular Technology Conference (VTC Spring), Dresden, Germany, 2–5 June 2013.
11. Zhang, R.; Zheng, Z.; Wang, M.; Shen, X.; Xie, L. Equivalent capacity in carrier aggregation-based LTE-A systems: A probabilistic analysis. *IEEE Trans. Wirel. Commun.* **2014**, *13*, 6444–6460. [CrossRef]

12. Khoramnejad, F.; Joda, R.; Sediq, A.B.; Abou-Zeid, H.; Atawia, R.; Boudreau, G.; Erol-Kantarci, M. Delay-Aware and Energy-Efficient Carrier Aggregation in 5G Using Double Deep Q-Networks. *IEEE Trans. Commun.* **2022**, *70*, 6615–6629. [CrossRef]
13. Nidhi; Mihovska, A.; Prasad, R. Overview of 5G New Radio and Carrier Aggregation: 5G and Beyond Networks. In Proceedings of the International Symposium on Wireless Personal Multimedia Communications (WPMC), Okayama, Japan, 19–26 October 2020.
14. Shajaiah, H.; Abdelhadi, A.; Clancy, T.C. Towards an application-aware resource scheduling with carrier aggregation in cellular systems. *IEEE Commun. Lett.* **2015**, *20*, 129–132. [CrossRef]
15. Joda, R.; Elsayed, M.; Abou-Zeid, H.; Atawia, R.; Sediq, A.B.; Boudreau, G.; Erol-Kantarci, M. QoS-aware joint component carrier selection and resource allocation for carrier aggregation in 5G. In Proceedings of the IEEE International Conference Communications, Montreal, QC, Canada, 14–23 June 2021.
16. Joda, R.; Elsayed, M.; Abou-Zeid, H.; Atawia, R.; Sediq, A.B.; Boudreau, G.; Erol-Kantarci, M. Carrier aggregation with optimized UE power consumption in 5G. *IEEE Netw. Lett.* **2021**, *3*, 61–65. [CrossRef]
17. Rostami, S.; Arshad, K.; Rapajic, P. Optimum radio resource management in carrier aggregation based LTE-Advanced systems. *IEEE Trans. Veh. Technol.* **2018**, *67*, 580–589. [CrossRef]
18. Li, J.; Han, Y. Optimal resource allocation for packet delay minimization in multi-layer UAV networks. *IEEE Commun. Lett.* **2017**, *21*, 580–583. [CrossRef]
19. Liu, F.; Zheng, K.; Xiang, W.; Zhao, H. Design and performance analysis of an energy-efficient uplink carrier aggregation scheme. *IEEE J. Sel. Areas Commun.* **2014**, *32*, 197–207.
20. Shajaiah, H.; Abdelhadi, A.; Clancy, T.C. A price selective centralized algorithm for resource allocation with carrier aggregation in LTE cellular networks. In Proceedings of the IEEE WCNC, New Orleans, LA, USA, 9–12 March 2015.
21. Zhang, R.; Zheng, Z.; Wang, M.; Shen, X.; Xie, L. Efficient coexistence of LTE with WiFi in the licensed and unlicensed spectrum aggregation. *IEEE Trans. Cogn. Commun. Netw.* **2016**, *2*, 129–140.
22. Peng, J.; Gao, Y.; Sun, X.; Zhan, W.; Guo, Z. 3GPP Fairness Constrained Throughput Optimization for 5G NR-U and WiFi Coexistence in the Unlicensed Spectrum. In Proceedings of the IEEE Wireless Communications and Networking Conference (WCNC), Austin, TX, USA, 10–13 April 2022.
23. Chiaraviglio, L.; Andreagiovanni, F.; Rossetti, S.; Sidoretti, G.; Blefari-Melazzi, N.; Salsano, S.; Chiasserini, C.-F.; Malandrino, F. Algorithms for the design of 5G networks with VNF-based reusable functional blocks. *Ann. Telecommun.* **2019**, *74*, 559–574. [CrossRef]
24. Huo, Y.; Dong, X.; Xu, W.; Yuen, M. Enabling multi-functional 5G and beyond user equipment: A survey and tutorial. *IEEE Access* **2019**, *7*, 116975–117008. [CrossRef]
25. Wang, L.; Fei, Z.; Zeng, M.; Li, B.; Huo, Y.; Dong, X.; Cui, Q. Spatial-Reuse-Based Efficient Coexistence for Cellular and WiFi Systems in the Unlicensed Band. *IEEE Internet Things J.* **2022**, *9*, 1885–1898. [CrossRef]
26. Iabal, J.; Illahi, U.; Khan, M.A.; Rauf, A.; Ali, E.M.; Bari, I.; Ali, H.; Khan, M.A.; Alibakhshikenari, M.; Dalarsson, M. A novel single-fed dual-band dual-circularly polarized dielectric resonator antenna for 5G Sub-6GHz applications. *Appl. Sci.* **2022**, *12*, 5222.
27. Renzo, M.D.; Lam, T.T.; Zappone, A.; Debbah, M. A Tractable Closed-Form Expression of the Coverage Probability in Poisson Cellular Networks. *IEEE Wirel. Commun. Lett.* **2019**, *8*, 249–252. [CrossRef]
28. Li, J.; Han, Y. Multi-RAT wireless network capacity optimization under optimal spectrum splitting in LTE-U. In Proceedings of the IEEE WCNC, Doha, Qatar, 3–6 April 2016.
29. Foss, S.G.; Zuyev, S.A. On a Voronoi Aggregative Process Related to a Bivariate Poisson Process. *Adv. Appl. Probab.* **1996**, *28*, 965–981. [CrossRef]
30. Zhang, S.; Zhang, H.; He, Q.; Bian, K.; Song, L. Joint Trajectory and Power Optimization for UAV Relay Networks. *IEEE Commun. Lett.* **2018**, *22*, 161–164. [CrossRef]
31. Andrew, J.G.; Baccelli, F.; Ganti, R.K. A tractable approach to coverage and rate in cellular networks. *IEEE Trans. Veh. Commun.* **2011**, *59*, 3122–3134. [CrossRef]
32. Jin, Z.; Kim, D.; Cho, J.; Lee, B. An Analysis on Optimal Cluster Ratio in Cluster-Based Wireless Sensor Networks. *IEEE Sens. J.* **2015**, *15*, 6413–6423. [CrossRef]
33. Boyd, S.; Vandenberghe, L. *Convex Optimization*; Cambridge University Press: Cambridge, UK, 2004.
34. Adan, I.; Resing, J. *Queueing Theory*; Department of Mathematics and Computer Science, Eindhoven University of Technology: Eindhoven, The Netherlands, 2001.

Disclaimer/Publisher's Note: The statements, opinions and data contained in all publications are solely those of the individual author(s) and contributor(s) and not of MDPI and/or the editor(s). MDPI and/or the editor(s) disclaim responsibility for any injury to people or property resulting from any ideas, methods, instructions or products referred to in the content.